Virchows Arch (1995) 426:401–410

ORIGINAL ARTICLE

Akihiro Hemmi · Akira Komiyama · Shinichi Ohno
Yasuhisa Fujii · Akira Kawaoi · Ryohei Katoh
Koichi Suzuki

Different organization of intermediate filaments in columnar cells of rat large intestinal mucosa as revealed by confocal laser scanning microscopy and quick-freezing and deep-etching method

Received: 10 November 1994 / Accepted: 27 January 1995

Abstract The relationship between cell differentiation and ultrastructural changes of intermediate filaments (IF) was studied in columnar cells of large intestinal mucosa of rats by confocal laser scanning microscopy and quick-freezing and deep-etching method. A feature of the IF in immature columnar cells was minibundle formation with prominent branching, which organized the meshwork structures. The minibundles, which appeared to be formed by the attachment of two or more IF in side-to-side fashion, were loosely distributed throughout the cytoplasm. In contrast, in mature columnar cells, the IF were densely distributed under the terminal web in the cytoplasm and beneath the upper part of the lateral membrane regions, whereas the other areas of the cytoplasm contained only a small number of IF. Minibundle formation was not observed, and the branching was rarely identified. The changes in the distribution and density of IF, which are expressed in specific areas of mature columnar cells, apparently represent a characteristic of intracellular differentiation. It is suggested that the dissociation of minibundled IF, which was often observed in the immature columnar cells, is an important step in the acquisition of functional polarity in cells of this type.

Key words Intermediate filament · Columnar cell · Large intestine · Laser microscopy · Deep-etching

Introduction

Many types of epithelial cells are characterized by the expression of different keratin proteins, which belong to intermediate filaments and form some parts of the cytoplasmic cytoskeleton. Many subtypes of keratin intermediate filament (IF) have been identified in various epithelial tissues through biochemical studies. They are encoded by different genes, and different epithelial cells express various subtypes of keratin IF [8, 12, 14, 25]. Furthermore, it has become clear that keratin IF are related to the differentiation and/or maturation of many epithelial cells [2, 3, 8, 11, 18, 19, 26, 32]. In the colonic mucosa, the expression of different subtypes of keratin IF during the course of epithelial cell differentiation has been detected by immunohistochemical studies [4, 7]. However, the ultrastructure of IF during the course of epithelial differentiation has not yet been studied in the colonic mucosa.

With the recent development of confocal laser scanning microscopy (CLSM) and its practical application in morphological research, it is now possible to examine optical section preparations even in thick specimens. CLSM also offers improved elimination of out-of-focus noise and greater resolution than conventional fluorescence microscopy [33]. The quick-freezing and deep-etching (QFDE) method is a morphological technique by which the ultrastructure of cytoskeletons and cell organelles in cells and tissues can be observed three-dimensionally at high resolution [1, 15, 20, 21, 27, 28]. It is well known that the cytoskeleton cannot be clearly observed using transmission electron microscopy with conventional Epon-embedded specimens, because the plastic embedding material interferes with its visualization. In the present study, we used CLSM combined with QFDE to investigate the differentiation-related changes of IF in the columnar epithelial cells of the rat large intestinal mucosa. As the marker of the IF observed by CLSM, several types of antibodies to keratin were used for the immunofluorescent staining. We now report the differentiation-related changes of the keratin IF that we observed using these recently developed techniques.

A. Hemmi (✉) · A. Komiyama · A. Kawaoi · R. Katoh
K. Suzuki
Second Department of Pathology, Yamanashi Medical University,
1110 Shimokato, Tamaho-cho, Nakakoma-gun,
Yamanashi 409-38, Japan

S. Ohno · Y. Fujii
Department of Anatomy, Yamanashi Medical University,
1110 Shimokato, Tamaho, Yamanashi 409–38, Japan

Materials and methods

Male Wistar rats, weighing 200–250 g, were anaesthetized with diethyl ether and sacrificed. Small segments of the large intestine (caecum) were removed and fixed for 24 h at 4°C with 4% paraformaldehyde in 0.1 M phosphate buffer (PB), at pH 7.4, or 95% methanol, respectively. They were treated with a graded series of sucrose concentrations in PB to minimize ice crystal artefacts. They were embedded in Tissue-Tek II OCT compound (Miles, USA), and then frozen in liquid nitrogen. Sections were cut at 10 μm for immunohistochemical study.

For the keratin immunostaining, wide-spectrum rabbit polyclonal anti-keratin antibody (Dako, Denmark; 1:200 dilution) was used as the first antibody for paraformaldehyde-fixed specimens, and mouse monoclonal anti-keratin 8 antibody (Chemicon International, USA) and mouse monoclonal anti-keratin 19 antibody (Chemicon; each 1:600 dilution) were used for 95% methanol-fixed specimens. FITC-conjugated anti-rabbit, or anti-mouse immunoglobulin (Dako) at a dilution of 1:50 was used as the second antibody. In addition, F-actin staining was performed using rhodamine-phalloidin (Molecular Probes, USA) at a dilution of 1:500. In most sections, double fluorescent staining with keratin and F-actin facilitated evaluation of the keratin-positive areas in the cytoplasm. Thus, mixtures of anti-keratin antibody and rhodamine-phalloidin were prepared for the double fluorescent staining. The first incubation step for keratin or F-actin was performed at room temperature for 3 h, and followed by the second incubation step, at room temperature for 1 h. These specimens were examined with a confocal laser scanning microscope (Olympus LSM-GB 200, Japan).

For QFDE studies the following procedure was followed. The large intestine of anaesthetized male Wistar rats (200–250 g) was perfused with 2% paraformaldehyde in PB via the heart. Small segments of the large intestine (caecum) were opened and gently rinsed with PB to remove the intestinal contents. The opened flat segments were cut into several pieces (3×5 mm) with sharp razor blades. These tissues were separated into two groups. For removal of soluble substances from the cytoplasm, the large intestinal tissues in each group were washed in PB with or without 0.5% saponin for 30 min. They were postfixed with 0.25% glutaraldehyde in PB for 30 min and rinsed in 10% methanol to minimize ice crystal formation during the subsequent quick-freezing step. The segments were placed on a copper metal holder with the mucosal side up and blotted with filter paper to remove excess fluid. They were then quickly frozen by the metal contact method using a quick-freezing machine (JEOL JFD-RFA, Japan), in which the copper metal is cooled in liquid nitrogen (-196°C). They were fractured in the liquid nitrogen with a scalpel to expose well-preserved surface areas [27, 28] and transferred into an EIKO FD-3AS etching machine (Eiko Company, Ibaragi, Japan). They were deeply etched under vacuum conditions ($1\sim4\times10^{-7}$ Torr) at -95°C for 10–20 min and rotary shadowed with platinum at the angle of 30°and with carbon at the angle of 90°. One drop of 2% collodion in amyl acetate was placed onto each replica as soon as the specimens were removed from the machine, to prevent breaking of the replicas into pieces during the subsequent digestion procedures. The replicas coated with dried collodion were floated on household bleach (Haiter, Kao, Japan) for 15–30 min to dissolve the cellular components. The replica membranes were washed in distilled water and cut into small pieces with a pair of scissors. They were mounted on Formvar-filmed copper grids and immersed in amyl acetate solution to dissolve the dried collodion. All replicas were observed in an electron microscope (Hitachi H-600), and photographed at various magnifications. Electron micrographs were printed from inverted negative films. For morphometric analysis, the diameter was measured at randomly selected areas of 460 IF under an Olympus SP 500, excluding those at the fractured margin of the filaments, and the distribution of diameters was represented as a histogram.

For further investigation of an effect of saponin extraction, the saponin-treated and quick-frozen large intestinal tissues were prepared for the cryosubstitution method. The frozen tissues were placed in acetone containing 2% OsO_4, and kept at about -80°C for 20 h [29]. The temperature of the samples was then raised, firstly to -20°C for 2 h, then to 4°C for 2 h and finally to room temperature. They were washed twice in absolute acetone and embedded in Epon 812. Ultrathin sections were cut with an ultramicrotome and doubly stained with uranyl acetate and lead citrate. All ultrathin sections were observed in an electron microscope (Hitachi H-600).

For conventional ultrathin section preparation, large intestinal tissues (caecum) were prefixed with 2.5% glutaraldehyde in PB for 24 h, and postfixed with 1% osmium tetroxide in PB for 1 h. They were routinely dehydrated in a graded ethanol series and embedded in Epon 812.

Results

Confocal laser scanning microscopy

A low-power view of the colonic mucosa after double fluorescent staining of rabbit polyclonal anti-keratin antibody and rhodamine-phalloidin is shown in Fig. 1a. Positive staining for keratin and F-actin was recognized as yellow-green and red signals, respectively. The former was observed in the cytoplasm of the mucosal epithelium, whereas the latter was observed at the apical surface and the baso-lateral cell boundary of the epithelial cells, in addition to the stromal cells in the lamina propria and smooth muscle cells in muscularis mucosa. The staining intensity of the keratin gradually increased with the migration distance of columnar cells from the crypt base to the mucosal surface. Gradual changes of staining areas and intensities were also observed in the cytoplasm.

In the mature columnar cells on the mucosal surface (Fig. 1b), intense keratin staining was observed in the cytoplasm beneath F-actin-positive areas of the apical surface and beneath the upper lateral cell membrane. There was weak staining with a reticulate pattern in the other areas of the cytoplasm. In contrast, in the immature columnar cell at the basal parts of the crypt (Fig. 1c), slight keratin staining with a reticulate pattern was observed throughout the entire cytoplasm.

In contrast to the staining pattern using the rabbit polyclonal anti-keratin antibody, keratin staining for mouse monoclonal anti-keratin 8 and anti-keratin 19 antibodies shows equal intensity throughout the crypt base to mucosal surface. In both mature and immature columnar cells, intense keratin staining was observed at an apical surface compared with the other areas of cytoplasm (Fig. 1d).

Some endocrine cells showed prominent keratin staining compared with that of the goblet or columnar cells (Fig. 1a, c), which was demonstrated by double staining of keratin immunostaining and Grimelius staining [16] (Fig. 1e, f). In a high-power view of the endocrine cells, positive staining of thick tonofilament-like bundles was seen in the supranuclear cytoplasm (Fig. 1g). In the goblet cells, the theca on the apical cytoplasm was not stained with keratin antibodies or rhodamine-phalloidin (Fig. 1b, c). These findings allowed us to distinguish them from the columnar cells.

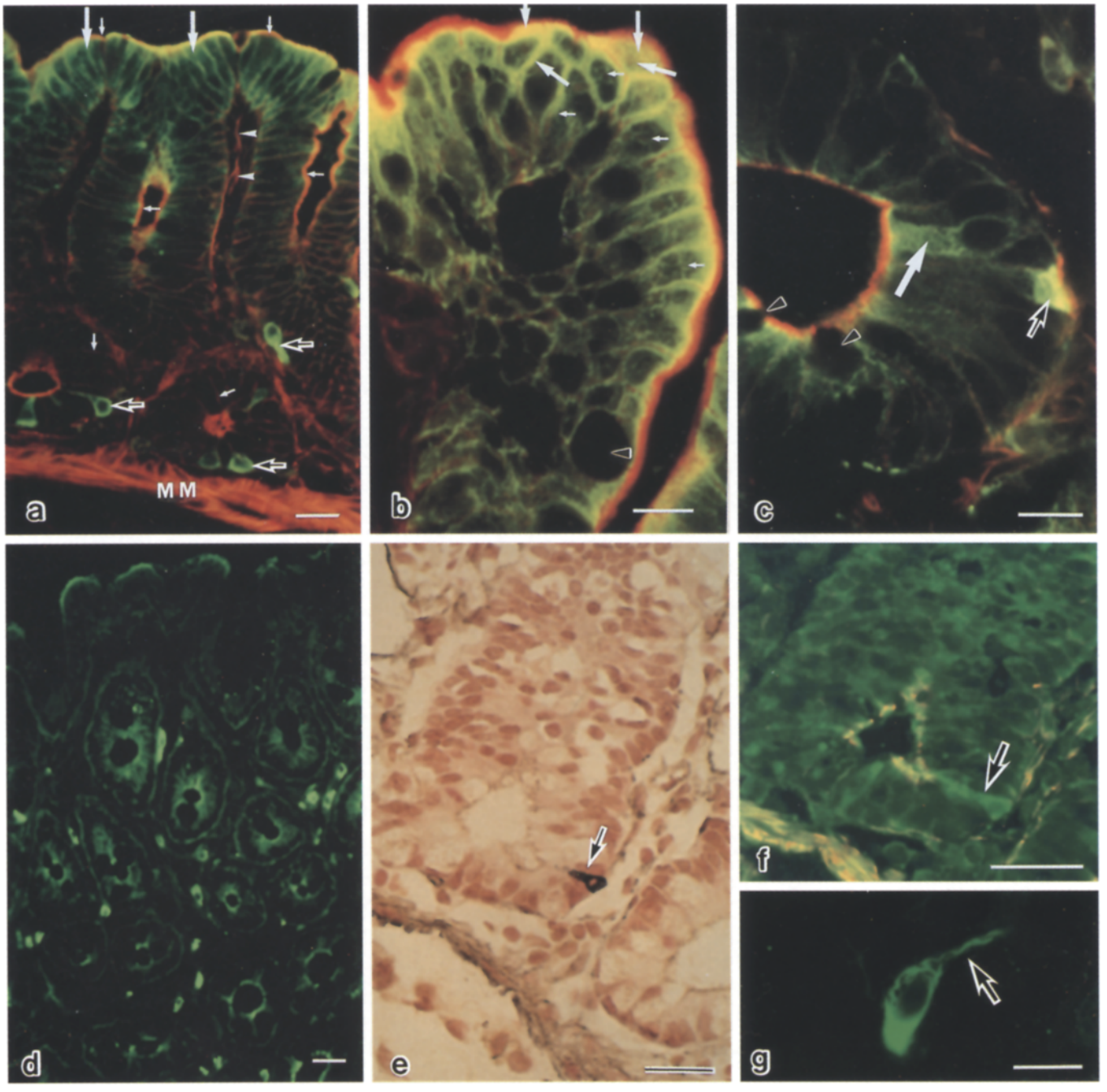

Fig. 1a–g Micrographs of the large intestinal mucosa. **a–c** Double-fluorescent stainings using polyclonal anti-keratin and rhodamine-phalloidin. Keratin and F-actin staining are recognized as yellow-green and red signals, respectively. **a** Positive staining for keratin is noted in the epithelial cells (*large arrows*). Positive staining for F-actin is observed at the apical surface and baso-lateral boundary of the epithelial cells (*small arrows*) and also in the stromal cells of the lamina propria (*arrowhead*) and the smooth muscle cells of the muscularis mucosa (*MM*). Low-power view; *bar* 20 μm. **b** Mucosal surface. Intense keratin staining is seen beneath the F-actin positive areas of the apical surface and the upper lateral cell membranes (*large arrows*). The other areas of the cytoplasm are weakly positive for keratin (*small arrows*). High-power view: *bar* 10 μm. **c** Crypt base. Positive staining for keratin is present throughout the entire cytoplasm of immature columnar cells (*large arrow*). High-power view; *bar* 10 μm. **d** Single immunofluorescent staining with anti-keratin 8. Positive staining for keratin 8 is observed mainly at the apical surface in the epithelial cells throughout crypt base to the mucosal surface. *Bar* 20 μm. Endocrine cells (*black arrows*) with intense keratin staining are seen (**a**, **c**). The theca of the goblet cell (*black arrowhead*) is not stained with keratin or F-actin (**b**, **c**). **e**, **f** Triple stainings using polyclonal anti-keratin, rhodamine-phalloidin and Grimelius method. Grimelius-positive endocrine cell (*black arrows*) reveals intense keratin staining. *Bar* 25 μm. **g** Single immunofluorescent staining using polyclonal anti-keratin. Positive staining of wavy bundle pattern (*black arrow*) is seen in the supranuclear cytoplasm of the endocrine cells. *Bar* 10 μm

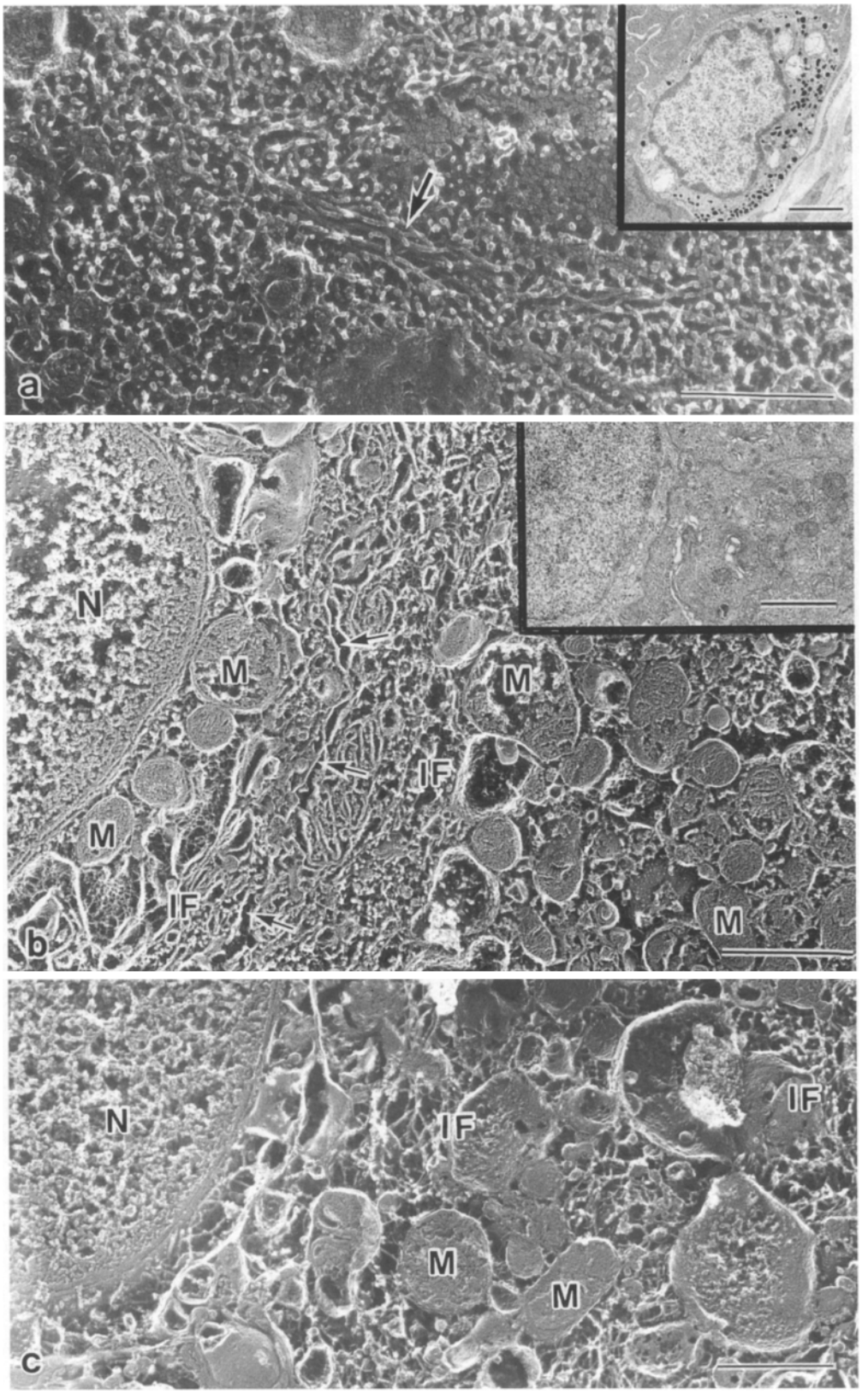

Fig. 2a–c Replica electron micrographs of **a** endocrine cells and **b, c** columnar cells. **a** Thick tonofilament-like bundle (*arrow*) of intermediate filaments is seen. *Bar* 0.5 μm. *Inset* Ultrathin section of endocrine cells. *Bar* 2 μm. **b, c** Replica electron micrographs of the columnar cell from **b** saponin-treated and **c** saponin-untreated samples. Intermediate filaments (*IF*), many mitochondria (*M*), other organelles, and a nucleus (*N*) are also seen. The lateral cell boundary (*arrow*) is recognized (*b*). **b, c** *Bar* 1 μm. *Inset* Corresponding areas in ultrathin section (*b*). *Bar* 2 μm

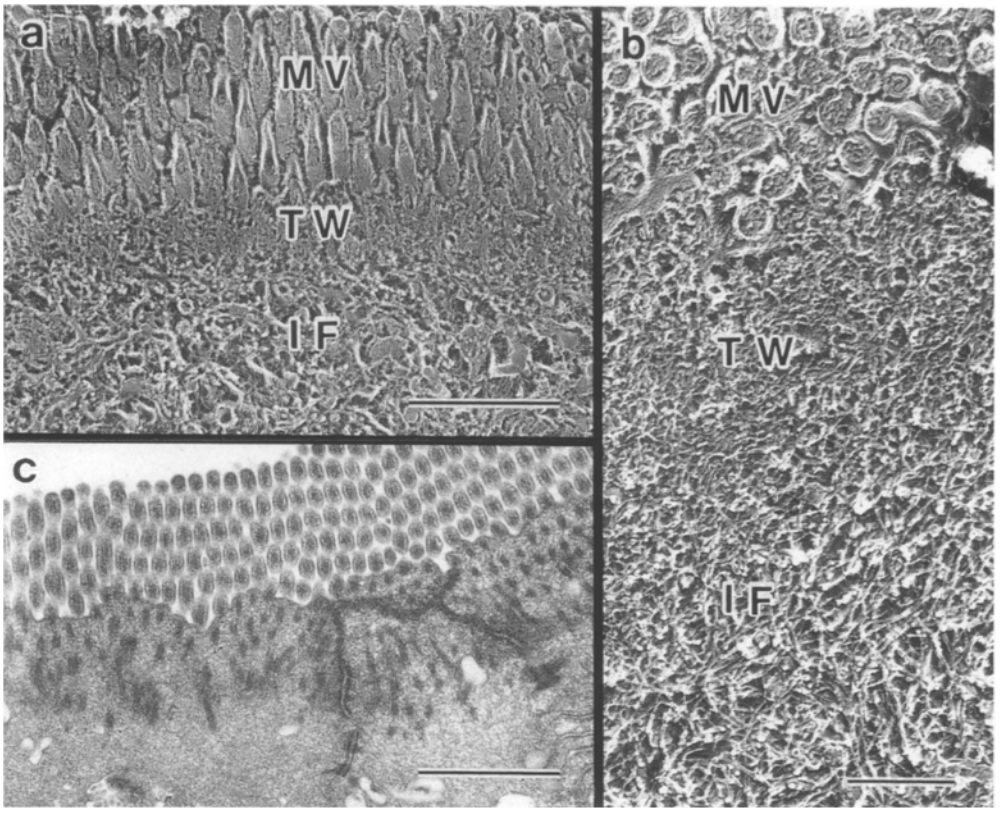

Fig. 3a–c Electron micrographs of the apical parts of mature columnar cells. **a, b** Obliquely or transversely fractured cell surfaces of replicas from saponin-treated sample. *Bars* 1 μm. **c** Corresponding areas in ultrathin section. *Bar* 0.5 μm. A dense tangle of intermediate filaments (*IF*) is seen under the terminal web region (*TW*). Microvilli (*MV*) are present on the apical surface

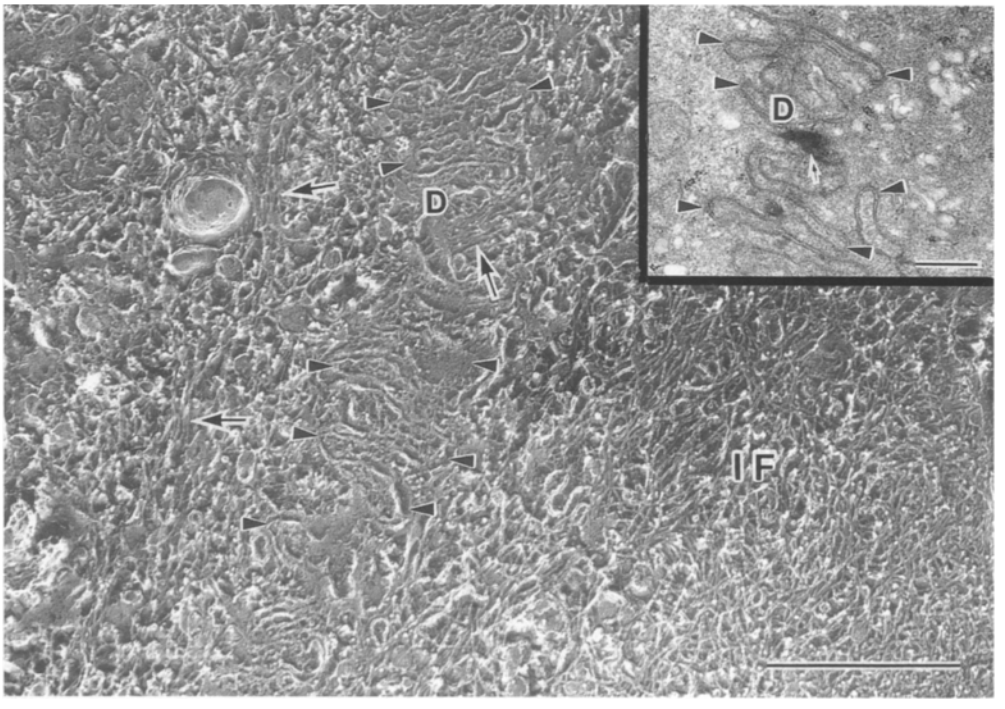

Fig. 4 Replica electron micrograph of the upper regions of the lateral cell boundary in a mature columnar cell from saponin-treated sample. IF-rich areas (*IF*) are noted in the cytoplasm beneath the cellular interdigitation (*arrowheads*). Tonofilament-like bundles (*arrows*) are occasionally observed. *Bar* 1 μm. *Inset* corresponding areas in ultrathin section. *Bar* 0.5 μm (*D* desmosome)

QFDE method

Images of cell organelles and cytoskeletal components in replica membranes were examined by comparing them with the findings for ultrathin sections obtained from the conventional method or the quick-freezing and cryosubstitution method. In the replica specimens, endocrine or goblet cells could be distinguished from columnar cells based on the following criteria. Endocrine cells were usually located on the basement membrane of the crypts, showed round and trigonal shapes, and contained specific secretory granules in the subnuclear cytoplasm and conspicuous thick tonofilament-like bundles of IF (Fig. 2a). Goblet cells were identified by the presence of

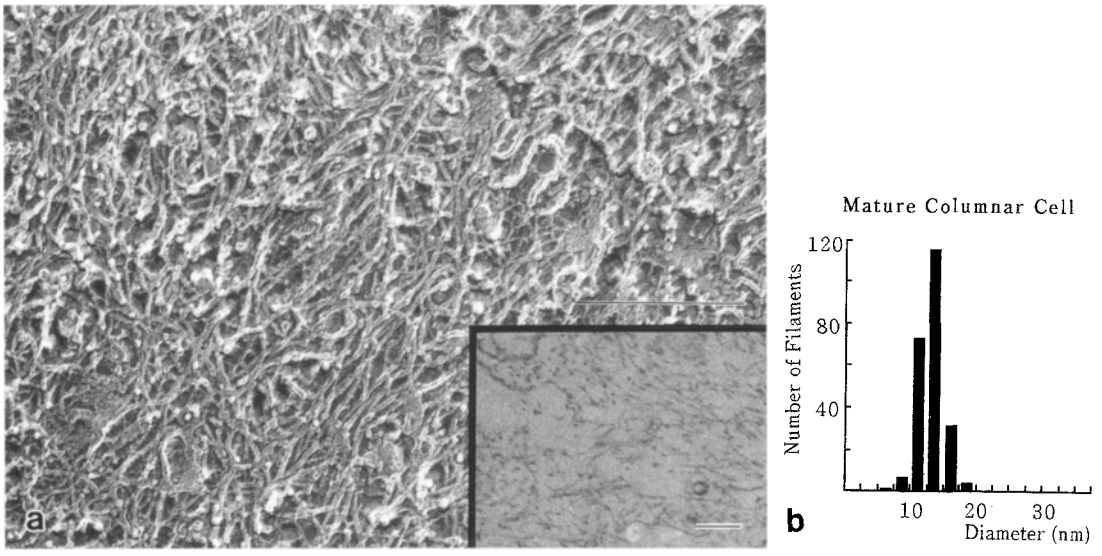

Fig. 5a, b Highly magnified replica micrograph of intermediate filaments in the cytoplasm under the terminal web region of a mature columnar cell (**a**) and the histogram of the frequency of IF (n=230) of each diameter (**b**). **a** There are numerous IF, but their size is relatively uniform. *Bar* 0.5 μm. *Inset* Corresponding areas in ultrathin section prepared by the quick-freezing and cryosubstitution method. *Bar* 0.1 μm. **b** Monophasic distribution of diameters, with the peak at 12.5–15.0 nm, is observed

the apical theca, mucigen granules and well-developed rough surface endoplasmic reticulum in their cytoplasm.

In order to determine the effects of saponin treatment, the ultrastructure of the saponin-untreated samples was compared with that of saponin-treated material. The inability to extract soluble intracytoplasmic proteins in the former material meant that cytoplasm of good quality for examination was restricted to small areas of the columnar cells. However the findings in the cytoskeleton and organelles were essentially the same in both samples (Fig. 2b, c).

Mature columnar cells

In mature columnar cells, the distribution and density of IF were uneven, depending on parts of the cytoplasm. A dense tangle of IF was observed under the terminal web

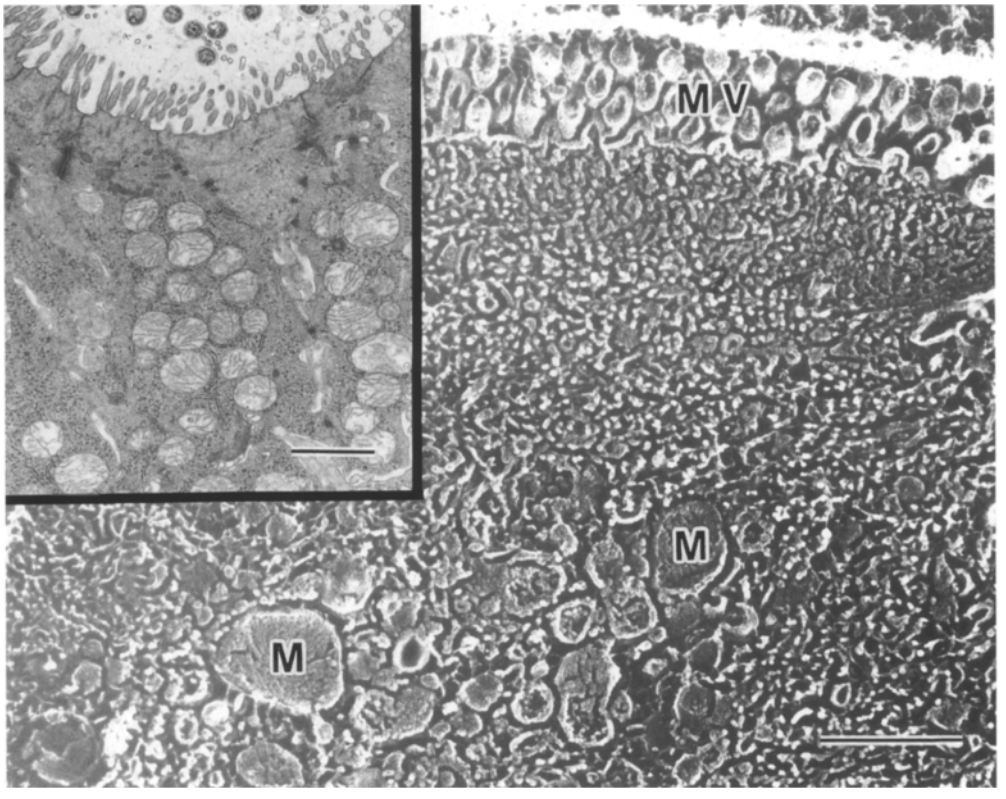

Fig. 6 Replica electron micrograph of the upper half of an immature columnar cell from saponin-treated sample. The microvilli (*MV*) on the apical surface of this cell are less developed than those shown in Fig. 3. Round mitochondria (*M*) are seen in the cytoplasm. *Bar* 1 μm. *Inset* Corresponding areas in ultrathin section. *Bar* 1 μm

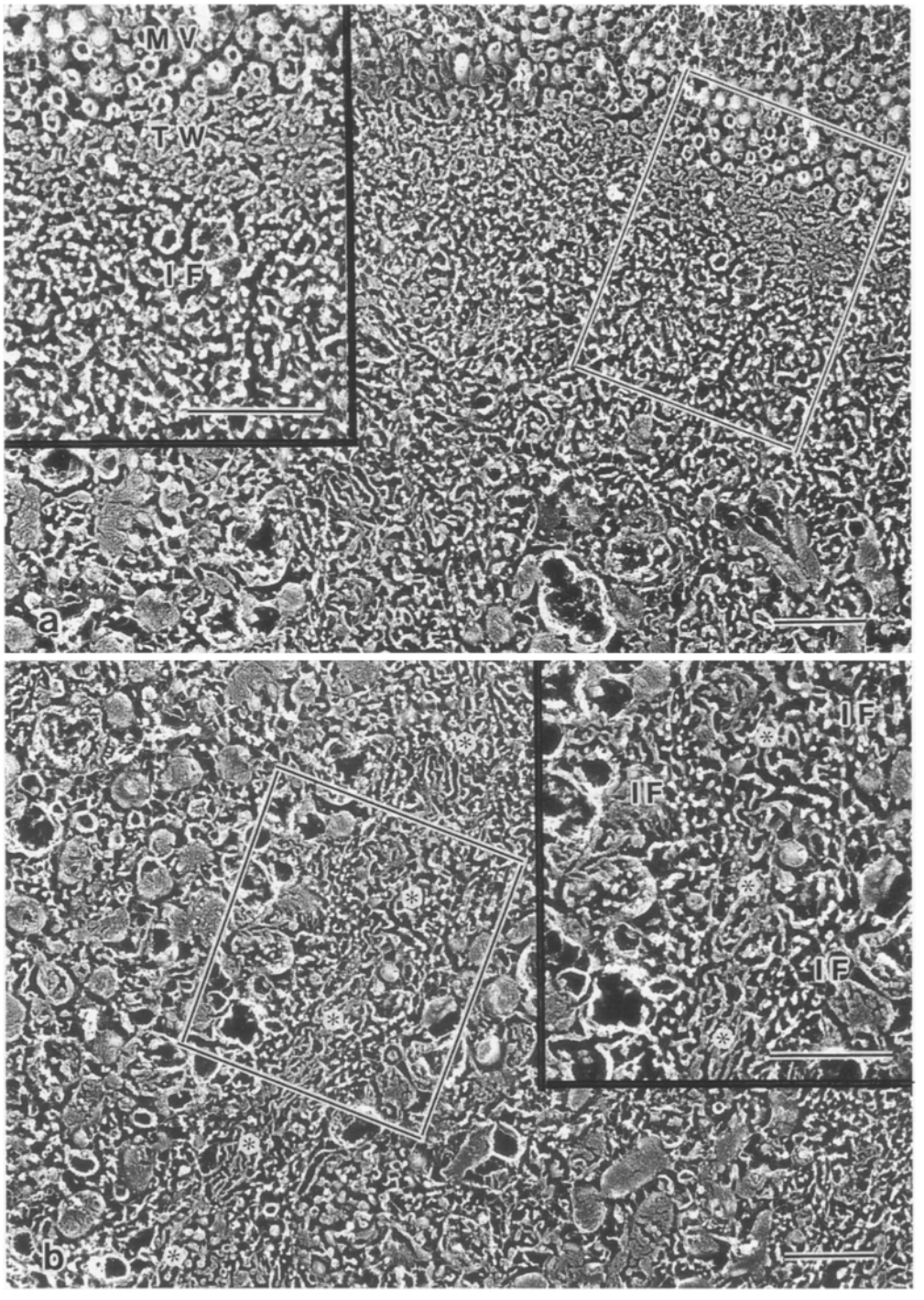

Fig. 7a, b Replica electron micrographs of immature columnar cells from saponin-treated sample. **a** Obliquely freeze-fractured surface of the apical cytoplasm. **b** Transversely fractured surface of the upper region of the lateral cell boundary. *Insets* Highly magnified views of the framed areas shown in **a** and **b**. The intermediate filaments (*IF*) are loosely distributed in the cytoplasm under the terminal web regions (*TW*) (**a**) and beneath the upper lateral membrane region (**b**). *Asterisks* indicate cell boundary (*MV* microvilli). *Bar* 1 μm

zone, which consisted of actin-like filaments with 5–10 nm in diameter (Fig. 3). Microvilli were observed on the apical surface. An IF-rich area was also noted in the upper lateral cytoplasm beneath the cellular interdigitation (Fig. 4). Most IF were randomly organized, but some showed tonofilament-like arrangement, in which several filaments showed parallel running course. These tonofilament-like bundles were frequently anchored at desmosomes located at the lateral cell membrane (Fig. 4), but the similar bundles that were not associated with the desmosomes were occasionally recognized in the cytoplasm. The other areas of the cytoplasm including perinuclear areas contained only a small number of IF, as shown in Fig. 2b.

In all areas of the cytoplasm, the IF formed long fibrous structures with straight or slightly wavy pattern (Fig. 5a). Branching and interconnection of these filaments were less frequently observed than in the immature columnar cells. A similar feature in IF formation was observed in the ultrathin sections of the saponin-treated sample prepared by the quick-freezing and cryosubstitution method (Fig. 5a, inset). The histogram of fil-

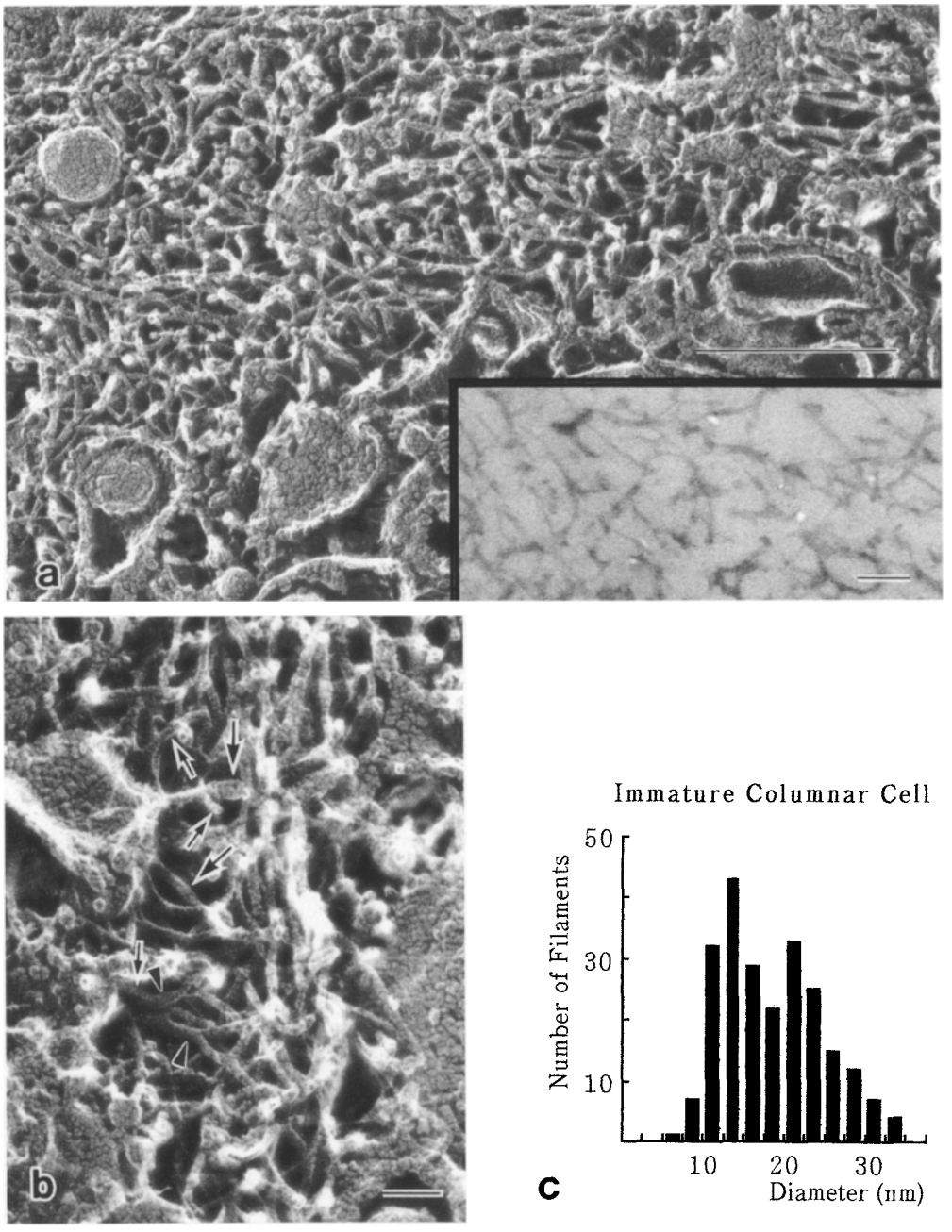

Fig. 8a–c Highly magnified replica micrographs of the intermediate filaments in the cytoplasm under the terminal web region of immature columnar cells obtained from saponin-treated sample (**a**, **b**) and the histogram of the frequencies of IF (n=230) of each diameter (**c**). **a** The intermediate filaments are loosely arranged with branching and interconnection. *Bar* 0.5 μm. *Inset* Corresponding area of ultrathin section prepared by the quick-freezing and cryosubstitution method. *Bar* 0.1 μm **b** The IF are roughly divided into thin (*small arrows*) and thick filaments (*large arrows*). Side-to-side attachments of two thin filaments are seen (*arrowheads*). *Bar* 0.1 μm. **c** A biphasic distribution, with peaks at 12.5–15.0 nm and 20.0–22.5 nm, is observed

ament thickness revealed monophasic pattern with a peak diameter of 12.5–15.0 nm (Fig. 5b).

Immature columnar cells

Compared with those in the mature cells, the mitochondria in the immature columnar cells were larger and rounder, and the microvilli were thicker and fewer in number (Fig. 6), as already reported elsewhere [23]. The IFs were loosely distributed throughout the cytoplasm (Fig. 7a, b). No tonofilament-like bundle of IF was observed in the cytoplasm.

In contrast to those in the mature cells, the IF in the immature columnar cells formed meshwork structures with prominent branching and interconnection (Fig. 8a). These filaments in the meshwork were roughly divided into thin and thick filaments, in which side-to-side attachments of two thin filaments were occasionally seen (Fig. 8b). This minibundle formation was observed from the replica membranes of the saponin-treated samples, as well as of the saponin-untreated samples. The distance between branching points on the same IF was shorter than that of the IF in the mature cells. A short branching structure in thin and thick filaments was occasionally seen in the ultrathin section from the saponin-treated sample, prepared by the quick-freezing and cryosubstitution method (Fig. 8a, inset). The histogram for the filament diameter showed biphasic pattern, with peaks at 12.5–15.0 nm and 20.0–22.5 nm (Fig. 8c).

Discussion

In the differentiation process of columnar epithelial cells in the large intestinal mucosa, the undifferentiated cells in basal parts of the crypt are known to migrate apically, and fully differentiated cells become detached from the most apical portion of the surface mucosa [6]. In the present study, we investigated the relationship between columnar cell differentiation and morphological changes of the IF in the large intestinal mucosa of rats. We found not only alteration of the distribution and density of the IF, but also changes in the patterns of branching and interconnection between IF. The IF have been defined as long and unbranched filaments 8–12 nm in diameter, which is intermediate between that of actin-containing microfilaments (5–6 nm) and that of microtubules (20–26 nm) [22]. The IF in the replica membranes showed slightly greater diameters (10–14 nm), because of the platinum metal shadowing. However, it seems likely that the general features of the IF in mature columnar cells are similar to those generally described for IF. The number of IF was increased beneath the terminal web regions and in the cytoplasm beneath the upper lateral membranes, while the other areas of the cytoplasm contained far fewer IF.

In immature columnar cells, thick filaments were observed in the meshwork structure formed of bundled IF as a result of the attachment of two or more filaments in a side-to-side fashion. This minibundle formation was not the tonofilament-like arrangement of IF. In the tonofilament-like bundle of IF, no filament was attached and the bundle consisted of many IF. Compared with those of the mature cells, tonofilament-like bundles were rarely observed in the immature cells. The distance between the branching points along the IF in the immature cells was shorter than that in the mature cells. In the immature cells, the filamentous structures were loosely arranged throughout the entire cytoplasm. In the present study, although the possibility remained that the minibundle formation of the IF was an artefact of the saponin treatment, the findings of the IF in the replica membrane with saponin-treated samples revealed similar features to those of the saponin-untreated samples, and to the ultrathin section of saponin-treated large intestinal tissues prepared by the quick-freezing and cryosubstitution method.

Although the meshwork structures in the immature columnar cells contained minibundles of IF, microtubules were rarely identified in any area of the cytoplasm. It has been reported that the microtubules in the columnar cells of the intestinal mucosa are not often preserved when prepared without taxol for QFDE [21, 30]. We consider that the paucity of microtubules we observed was probably due to the permeation and/or paraformaldehyde fixation without taxol, which preceded the quick-freezing step. For the preservation of the microtubules in the cells of the intestinal mucosa, a suitable stabilizer such as taxol is needed in the preparation steps for the QFDE method [31].

IF have been reported to be important in the stabilization of cell shape and integrity [24]. In addition to these functions, it is accepted that the genetic expression of IF is related to the differentiation and/or maturation of epithelial cells or tissues, such as the intestinal epithelium [4, 7] bile duct and liver cells [11, 32], mammary glands [2, 3], renal tubules and collecting ducts [18, 19, 26] and the epidermis of the skin [8]. Furthermore, a mosaic expression pattern of keratin 19-negative or -positive cells has been recognized in gastrointestinal epithelia, as well as in other simple epithelia [2–4]. The keratin 19-negative cells are thought to be precursor cells (undifferentiated cells) of the keratin 19-positive cells. It was also reported that the keratin 19-negative cells are frequently distributed in the areas where immature cells with proliferative potentiality are mainly localized, namely in the crypts of the small or large intestine and the gastric pits [4]. Moreover, they have higher proliferative potentiality than the keratin 19-positive cells, as revealed by culture studies of mammary luminal cells [2, 3, 5]. In an immunofluorescent study of the keratin on the human large intestinal mucosa, Chesa et al. [7] observed that the intensity of keratin immunostaining showed a gradual increase with columnar cell differentiation. In our findings of immunofluorescent staining using different anti-keratin antibodies for the rat large intestine, there were some differences in keratin staining patterns. This discrepancy suggests that columnar cell differentiation was accompanied by the expression of different subtypes of keratin IF, as reported elsewhere. However, to our knowledge there is no report of ultrastructural examination of the IF in columnar cells at various stages of differentiation in the large intestinal mucosa. Our study employing the CLSM and QFDE methods demonstrated that the stage of differentiation of columnar cells is related not only to the expression of different subtypes of keratin IF, but also to changes of the intracytoplasmic distribution and density of the IF.

Ultrastructure of keratin IF in small intestinal epithelia has been examined by immunofluorescence microscopy and transmission electron microscopy with ultrathin sections [13]. Hirokawa and Heuser [21] also reported the cytoskeletal ultrastructural findings for microvilli and terminal web regions in the small intestines observed using the QFDE method. Several other reports describe the distribution of the major cytoskeletal structures, such as microfilaments, IF and microtubules, as well as of cytoskeleton-associated proteins, including α-actinin, vinculin, fimbrin, villin, 110-kDa protein and myosin [9, 10, 17, 21]. However, most of these studies of columnar cells were usually performed using materials from the small intestine. Our results regarding the distribution of IF in the mature columnar cells of the large intestinal mucosa are very similar to the reported findings for these cells of the small intestine.

In conclusion, the morphology of IF in immature columnar cells differs from that of mature columnar cells, and this difference appears to be related to the stage of intracellular differentiation. In the stage of mature col-

umnar cells, the IF are localized densely in specific areas of the cytoplasm. It is therefore suggested that the dissociation of minibundled IF, which was often observed in the immature columnar cells, is an important step in the acquisition of functional polarity of cells of this type.

References

1. Baba T, Shiozawa N, Hotchi M, Ohno S (1991) Three-dimensional study of the cytoskeleton in macrophages and multinucleate giant cells by quick-freezing and deep-etching method. Virchows Arch [B] 61: 39–47
2. Bartek J, Durban EM, Hallowes RC, Taylor-Papadimitriou J (1985) A subclass of luminal epithelial cells in the human mammary gland defined by antibodies to cytokeratins. J Cell Sci 75: 17–33
3. Bartek J, Taylor-Papadimitriou J, Miller N, Millis R (1985) Patterns of expression of keratin 19 as detected with monoclonal antibodies in human breast tissues and tumours. Int J Cancer 36: 299–306
4. Bartek J, Bartkova J, Taylor-Papadimitriou J, Rejthar A, Kovarik J, Lukas Z, Vojtesek B (1986) Differential expression of keratin 19 in normal human epithelial tissues revealed by monospecific monoclonal antibodies. Histochem J 18: 565–575
5. Bartek J, Bartkova J, Taylor-Papadimitriou J (1990) Keratin 19 expression in the adult and developing human mammary gland. Histochem J 22: 537–544
6. Chang WWL, Leblond CP (1971) Renewal of the epithelium in the descending colon of the mouse. I. Presence of three cell populations: vacuolated-columnar, mucous and argentaffin. Am J Anat 131: 73–100
7. Chesa PG, Rettig WJ, Melamed MR (1986) Expression of cytokeratins in normal and neoplastic colonic epithelial cells. Implications for cellular differentiation and carcinogenesis. Am J Surg Pathol 10: 829–835
8. Cooper D, Schermer A, Sun TT (1985) Classification of human epithelia and their neoplasms using monoclonal antibodies to keratins: strategies, applications, and limitations. Lab Invest 52: 243–256
9. Drenckhahn D, Franz H (1986) Identification of actin-, α-actinin-, and vinculin-containing plaques at the lateral membrane of epithelial cells. J Cell Biol 102:1843–1852.
10. Drenckhahn D, Dermietzel R (1988) Organization of the actin filament cytoskeleton in the intestinal brush border: a quantitative and qualitative immunoelectron microscope study. J Cell Biol 107: 1037–1048
11. Eyken PV, Sciot R, Desmet V (1988) Intrahepatic bile duct development in the rat: a cytokeratin-immunohistochemical study. Lab Invest 59: 52–59
12. Franke WW, Weber K, Osborn M, Schmid E, Freudenstein C (1978) Antibody to prekeratin. Decoration of tonofilament-like arrays in various cells of epithelial character. Exp Cell Res 116: 429–445
13. Franke WW, Appelhans B, Schmid E, Freudenstein C (1979) The organization of cytokeratin filaments in the intestinal epithelium. Eur J Cell Biol 19: 255–268
14. Franke WW, Schiller DL, Moll R, Winter S, Schmid E, Engelbrecht I (1981) Diversity of cytokeratins. Differentiation specific expression of cytokeratin polypeptides in epithelial cells and tissues. J Mol Biol 153: 933–959
15. Furuta K, Ohno S, Gibo Y, Kiyosawa K, Furuta S (1992) Three-dimensional ultrastructure of normal rat hepatocytes by quick-freezing and deep-etching method. J Gastroenterol Hepatol 7:486–490
16. Grimelius L (1968) A silver nitrate stain for alpha-2 cells in human pancreatic islets. Acta Soc Med Upsal 73: 243–270
17. Hagen SJ, Trier JS (1988) Immunocytochemical localization of actin in epithelial cells of rat small intestine by light and electron microscopy. J Histochem Cytochem 36: 717–727
18. Hemmi A, Mori Y (1990) Immunohistochemical and scanning electron microscopic study of cytokeratin distribution in the collecting tubule of the rat kidney. Acta Pathol Jpn 40: 307–313
19. Hemmi A, Mori Y (1991) Immunohistochemical study of cytokeratin distribution in the collecting duct of the human kidney. Acta Pathol Jpn 41: 516–520
20. Heuser JE, Kirschner MW (1980) Filament organization resolved in platinum replicas of freeze-dried cytoskeleton. J Cell Biol 86: 212–234
21. Hirokawa N, Heuser JE (1981) Quick-freeze, deep-etch visualization of the cytoskeleton beneath surface differentiations of intestinal epithelial cells. J Cell Biol 91: 399–409
22. Ishikawa H, Bischoff R, Holtzer H (1968) Mitosis and intermediate-sized filaments in developing skeletal muscle. J Cell Biol 38: 538–555
23. Larenzsonn V, Trier JS (1966) The fine structure of human rectal mucosa. The epithelial lining of the base of the crypt. Gastroenterology 35: 88–101
24. Lazarides E (1980) Intermediate filaments as mechanical integrators of cellular space. Nature 283: 249–256
25. Moll R, Franke WW, Schiller DL (1982) The catalog of human cytokeratins: patterns of expression in normal epithelia, tumors and cultured cells. Cell 31: 11–24
26. Moll R, Hage C, Thoenes W (1991) Expression of intermediate filament proteins in fetal and adult human kidney: modulations of intermediate filament patterns during development and in damaged tissue. Lab Invest 65: 74–86
27. Naramoto A, Ohno S, Furuta K, Itoh N, Nakazawa K, Nakano M, Shigematsu H (1991) Ultrastructural studies of hepatocyte cytoskeletons of phalloidin-treated rats by quick-freezing and deep-etching method. Hepatology 13: 222–229
28. Ohno S, Fujii Y (1991) Three-dimensional studies of the cytoskeleton of cultured hepatocytes: a quick-freezing and deep-etching study. Virchows Arch [A] 418: 61–70
29. Ohno S, Hora K, Furukawa T, Oguchi H (1992) Ultrastructural study of the glomerular slit diaphragm in fresh unfixed kidneys by a quick-freezing method. Virchows Arch [B] 61: 351–358
30. Sandoz D, Laine MC, Nicolas G (1985) Distribution of microtubules within the intestinal terminal web as revealed by quick-freezing and cryosubstitution. Eur J Cell Biol 39: 481–484
31. Schiff PB, Fant J, Horwitz SB (1979) Promotion of microtubule assembly in vitro by taxol. Nature 277: 665–667
32. Vassy J, Rigaut JP, Hill AM, Foucrier J (1990) Analysis by confocal scanning laser microscopy imaging of the spatial distribution of intermediate filaments in foetal and adult rat liver cells. J Microsc 157: 91–104
33. White JG, Amos WB, Fordham M (1987) An evaluation of confocal versus conventional imaging of biological structures by fluorescence light microscopy. J Cell Biol 105: 41–48